Poly(Vinyl Alcohol) Cellulose Nanocomposites

22

Qingzheng Cheng, Siqun Wang, and Zhaohui Tong

Contents

Q. Cheng (✉)
Forest Products Development Center, Auburn University, Auburn, AL, USA

Agricultural & Biological Engineering, University of Florida, Gainesville, FL, USA
e-mail: chenggq@hotmail.com

S. Wang
Center for Renewable Carbon, University of Tennessee, Knoxville, TN, USA
e-mail: swang@utk.edu

Z. Tong
Agricultural & Biological Engineering, University of Florida, Gainesville, FL, USA
e-mail: ztong@ufl.edu

Abstract

Cellulose is the most abundant natural biopolymer in the world. Cellulose fibrils in micro- and nanoscales are attractive materials to replace man-made fibers such as glass and aramid fibers. They can be used as the reinforced additives or fillers to produce environmentally friendly materials. Poly(vinyl alcohol) (PVA) is a biodegradable polymer, which has many advantages including the resistance to solvents, being able to chemically bond with cellulose and soluble in hot water. The water solubility of PVA allows it to be fabricated with other water-soluble materials (e.g., nanocellulose solution) to form a nanocomposite by film casting method. In the introduction of this chapter, we overviewed the recently developed methods to generate cellulose fibril in a micro- or nanoscale, the characterization of nanocrystals and nanofibers, and the fabrication methods for PVA/cellulose nanocomposites. As an example, commercial microfibrillated cellulose (MFC) was used to reinforce PVA through film casting method in this chapter. The morphologies and sizes of the MFC were detected by scanning electronic microscopy (SEM). The effects of MFC on mechanical and thermal properties and surface morphologies of composites were studied. The introduction of MFC increased both tensile modulus and tensile strength of neat PVA. The composite had a higher thermal degradation temperature compared to neat PVA. The SEM images indicated the existence of interbonding between PVA and cellulose fibrils.

1   Introduction

In the past decades, biodegradable products from renewable materials are becoming increasingly more attractive due to the escalating price of the crude oil and the shortage of petroleum resources. Cellulose, the most abundant natural biopolymer in the world, is synthesized in biomass through photosynthesis. The cellulosic fibers and their derivatives (e.g., fibrils in micro- and nanoscales, cellulose crystals/whiskers) have many advantages including biodegradable, renewable, relatively low cost and density, nonabrasive, and high specific strength and modulus. Therefore, these cellulosic materials are used as reinforced materials or fillers to produce environmentally friendly products.

Nano-sized materials (e.g., nanocellulose) are defined as the materials that have at least one dimension in a nanometer scale (1–100 nm) [1]. Microfibers are defined as the fibers with 0.1–1 μm in diameter and a corresponding minimum length of 5–50 μm [2]. Cellulose fibrils in micro- and nanoscales have much higher mechanical properties compared with original fibers [3, 4]. It is still very challengeable

for a low-cost process to isolate fibrils and to further fabricate nanocomposites with the improving strength and stiffness as expected. Chemical and mechanical processes are two common methods to obtain cellulose fibrils. Strong acid hydrolysis is one of the primary chemical methods that remove the amorphous regions of cellulose fibers to produce cellulose nanocrystals or nanowhiskers. The mechanical method utilizes strong shear forces to disintegrate cellulose fibers into fibril bundles. Many terms, including microfibrillated cellulose (MFC), cellulose nanocrystal, cellulose nanofibril, cellulose whisker, and cellulose nanofibers, have been used to describe different types of cellulosic fibrils in micro- and nanoscales. In this chapter, we use cellulose nanofibers for mechanically isolated fibrils and nanocrystals for chemical isolated fibrils after removing amorphous parts using strong acids. Bacterial cellulose fibrils can also be used to reinforce PVA, but it will not be discussed in this chapter [5, 6].

Poly(vinyl alcohol) (PVA) is a biodegradable polymer, which has many advantages including resistance to solvents, being able to chemically bond with cellulose. It is soluble in hot water, which enables the formation of films by first mixing water suspensions of PLA and cellulose nanofibers and nanocrystals followed by a casting process. PVA has also been broadly used as protective colloids in the manufacture of polymer emulsions, for bindings of pigments and fibers, and for the production of detergents and cleansing agents, adhesives, emulsion paints, and solution cast films [7, 8]. However, it has relatively low mechanical strength and integrity. Therefore, recently many researchers have focused on using cellulose nanofibers and nanocrystals to reinforce PVA to improve its mechanical and thermal properties.

This chapter will review the processes to isolate cellulose fibrils in micro- and nanoscales, the characteristics of recently developed cellulose fibrils, and the properties of its reinforced PVA nanocomposites in the introduction. As a comparison, commercial microfibrillated cellulose (MFC) was used to reinforce PVA as well. The morphologies and the average sizes of MFC were estimated by scanning electronic microscopy. The effects of MFC on mechanical and thermal properties and surface morphologies of the PVA nanocomposites were investigated.

1.1   The Isolation of Cellulose Nanocrystals by Chemical Methods

Strong acid hydrolysis, as one of the primary chemical methods, has been used to remove the amorphous regions of cellulose fibers and then generate cellulose nanocrystals, also called cellulose whiskers. Figure 22.1 shows typical chemical isolation procedures for the cellulose nanocrystal generation from raw lignocellulosic materials (wood residues or other biomass) and from other cellulosic materials. Generally, when raw lignocellulosic materials were used, the lignin and hemicellulose have to be removed before acid hydrolysis process [9–11]. After lignin removal, the procedure to prepare cellulose nanocrystals from pure cellulose
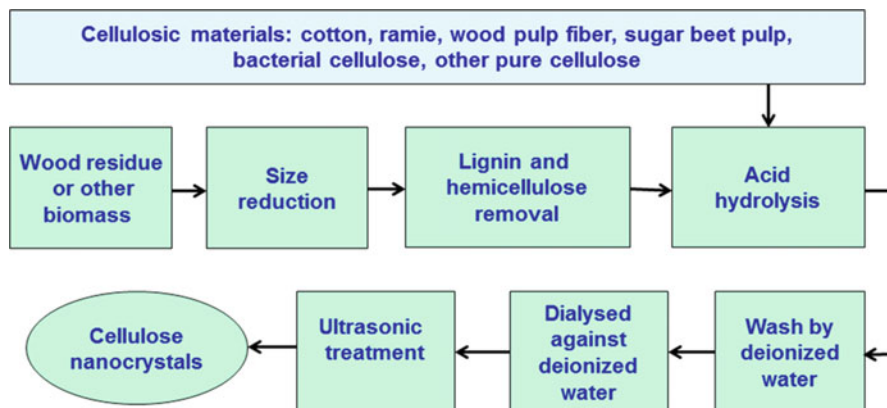
Fig. 22.1 Typical chemical isolation procedure of cellulose nanocrystals from wood residues or other biomass and from cellulose materials

normally includes five steps: acid hydrolysis, centrifugation and neutralization, washing with deionized water, further disintegration by ultrasonic treatment, and ultrafiltration to remove any remaining ions (Fig. 22.1) [11, 12]. Cellulose nanocrystals have been obtained from many cellulose materials, such as wood pulp fibers, cotton, ramie, tunicate mantles, sugar beet pulp, and bacterial cellulose [10, 13–26]. The properties and morphologies of cellulose nanocrystals are significantly affected by acid reaction conditions [17].

1.2   The Isolation of Cellulose Nanofibers by Mechanical Methods

The most common mechanical method utilizes strong shear forces, such as the shear force generating from a homogenizer, to disintegrate cellulose fibers to fibrils in a micrometer scale. This method can be used to generate cellulose microfibril or bundles, commonly called microfibrillated cellulose (MFC) [14, 27, 28]. A high-pressure refiner or super grinder treatment can also be used to generate cellulose nanofibers [18, 29]. Another method is a process that generates the shear force from high-intensity ultrasonication (HIUS). A HIUS processor can be used to isolate fibrils from several cellulosic resources, such as regenerated cellulose fiber, pure cellulose fiber, microcrystalline cellulose, and pulp fiber [30–32]. HIUS produces a very strong mechanical oscillating power from ultrasonic waves, which forms hydrodynamic forces to separate cellulose fibrils [33]. A mixture suspension of fibers and fibrils with a diameter ranging from tens of nanometers (nm) to microns (μm) was obtained after HIUS treatment. SEM and AFM images can be used to observe the structure and appearance of the regenerated cellulose fibrils isolated by HIUS (Figs. 22.2 and 22.3). The diameters of the fibrils were in a wide range of tens-to-hundreds nanometers and have a wide range of aspect ratios.
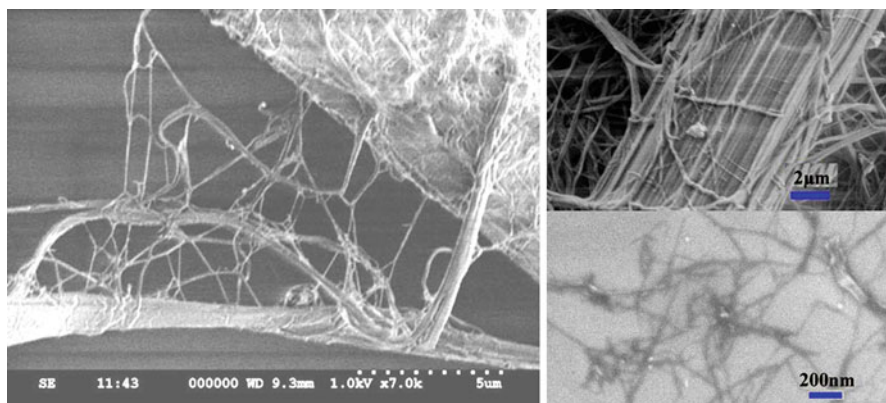
Fig. 22.2 SEM images of cellulose fibers and fibrils isolated by ultrasonic treatment (Reprinted from [31] with permission from Wiley)
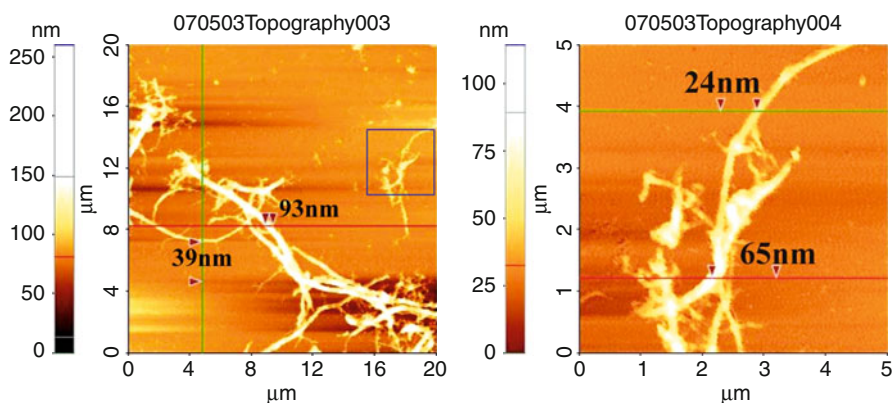

Fig. 22.3 AFM images of cellulose fibrils isolated by ultrasonic treatment (Reprinted from [31] with permission from Wiley)

1.3   Characterizations of Cellulose Nanocrystals and Nanofibers

Cellulose fibrils can be characterized by morphological observation, degree of fibrillation, crystalline measurement, and mechanical tests. Several technologies can be used for morphological observation, such as a scanning electron microscope (SEM), an atomic force microscope (AFM), and a transmission electron microscopy (TEM) [12, 16, 18, 34–36]. The degree of fibrillation of the cellulose fibers can be evaluated by water retention value (WRV) [27, 28, 30, 31, 37–39]. The crystallinity of the cellulose fibrils can be studied through wide-angle X-ray diffraction (WAXD) [2, 34, 38, 40] or Fourier transform infrared spectroscopy (FTIR) [31].
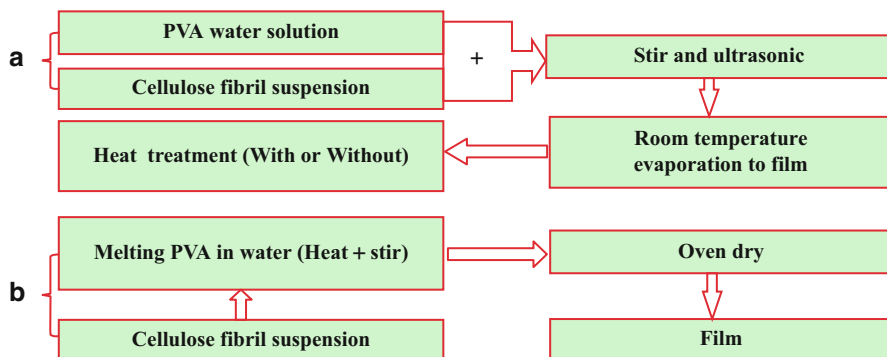
Fig. 22.4 Typical fabrication procedure of PVA cellulose nanocomposites: (**a**) PVA solution and cellulose fibril suspension mixture process, (**b**) cellulose fibril suspension added in melting PVA process

Mechanical properties, especially the elastic modulus of the crystalline region of cellulose, have been determined either experimentally or theoretically using Raman spectroscopy and X-ray diffraction [6, 13, 41, 42]. AFM three-point bending test can be used to measure mechanical properties of single cellulose nanofibers [3, 43–45].

1.4 Fabrication and Characterization of PVA Cellulose Nanocomposites

The most frequently used method for cellulose nanocomposite fabrication is solvent evaporation casting, using water-soluble and other solvent-soluble polymers. For example, cellulose nanocomposites can be produced by a solvent casting method in Teflon or propylene dishes [29, 46]. Nanocomposites can also be obtained through a hot-pressing method using freeze-drying fibrils [47]. An optically transparent composite reinforced with plant fiber-based cellulose microfibrils can be produced by a mat formation at first, followed by a resin immersion and curing by UV light [48], or followed by a hot press with high pressures [49], or compression molding [50].

The film casting method is a commonly used method that produces PVA cellulose nanocomposites because PVA is a hot-water-soluble polymer. Figure 22.4 shows two fabrication procedures for the formation of PVA cellulose nanocomposites. In procedure (a), PVA was dissolved in water under heating and then mixed with cellulose fibril suspension. Then the mixture was treated by untrasonification and followed by a film casting process [4, 38]. In procedure (b), PVA powder was dissolved in hot water under heating and continuous stirring at first. Then nanofiber suspension was added to the hot PVA solution and heated until the solution became viscous. The formed mixture solution was poured onto dishes and then heated in a 50 °C in an oven to cast films [36].
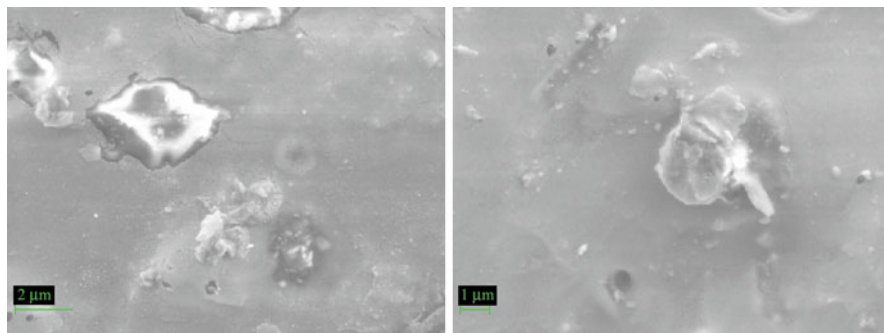
Fig. 22.5 SEM images of the fractured cross sections of PVA composites reinforced with small cellulose fibrils (Reprinted from [4] with permission from Elsevier)
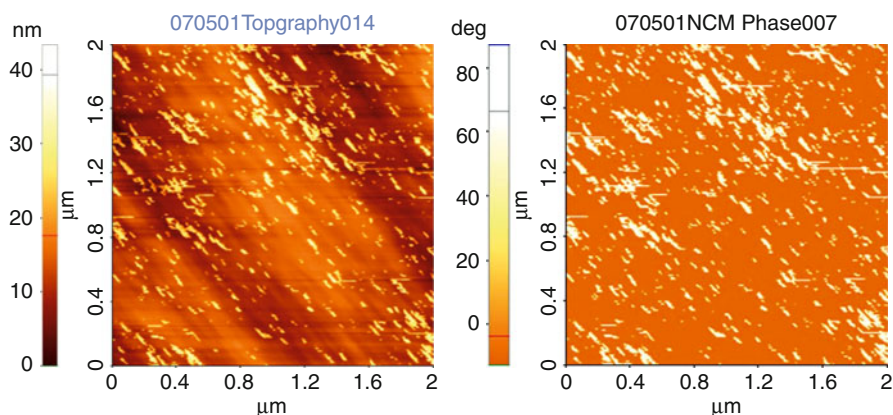

Fig. 22.6 AFM topography and phase images of the cross sections of PVA composites reinforced with small cellulose fibrils (Reprinted from [4] with permission from Elsevier)

Many instruments have been used to investigate the mechanical, morphological, and thermal properties of cellulose nanocomposites. The mechanical properties can be measured by tensile and bending tests [4, 5, 10, 12, 23, 24, 29, 34, 38, 49, 51–53]. Dynamic mechanical analysis (DMA) tests can also be used to evaluate composite performance under various conditions of temperature and relative humidity [12, 46, 53]. AFM, SEM, and TEM are common tools for morphological character-izations of nanocomposites [3, 16, 19, 21, 29, 32, 51]. Figures 22.5 and 22.6 show SEM images of fracture surfaces of nanocomposites after tensile testing and AFM images of cross sections after cutting by microtome from the PVA nanocomposites reinforced by a small number of cellulose fibrils. Differential scanning calorimetry (DSC), thermogravimetric analyzer (TGA), and DMA have been used to evaluate thermal properties of cellulose nanocomposites [10, 11, 22, 23, 25, 27, 32, 53–57].

2   Materials and Methods

2.1   Materials

Poly(vinyl alcohol) (PVA) was purchased from Acros Organics (99–100 % hydrolyzed, average M.W. 86000) and used as the matrix material in the composites. Microfibrillated cellulose (MFC, 10 % solid slurry, Daicel Chemical Industries Ltd., Japan) was used for PVA reinforcement.

The MFC morphological structure was observed by field emission gun-scanning electron microscopy (FEI XL-40 FEG-SEM, Tokyo, Japan). All samples were coated with Au-Pd ($\sim$10 nm) before the SEM observation and the operating voltage was 15 kV.

2.2   MFC Nanocomposite Fabrication

Solid PVA was dissolved in water to prepare the solution with 10 wt% of solid content under heating [4, 8]. MFC water suspension (1 wt%) and the PVA water solution (10 wt%) were mixed together and stirred manually and then treated by ultrasonification (Model 300 V/T, BioLogics, Inc., Manassas, VA) for 3 min at a power level of 50 % and under a continuous mode. The cellulose nanocomposites with four MFC loading levels (0 wt%, 2 wt%, 5 wt%, and 10 wt%) were fabricated by the film casting method. The mixtures were degassed in a desiccator using vacuum and then evaporated in Petri dishes at room temperature with relative humidity (RH) of $\sim$30 % until films were formed. The films were then heated in an oven at 70 °C for more than 4 h. The samples were kept in a desiccator with magnesium nitrate $Mg(NO_3)_2$ saturated solution (RH about 53 % at $\sim$22 °C) more than 3 days before mechanical and thermal properties were tested in accordance to ASTM D1708 conditioning conditions (RH is 50 $\pm$ 5 % and time is more than 40 h) [58]. The nominal thickness of the nanocomposite films was 127 μm.

2.3   Characterization of PVA and PVA MFC Nanocomposites

An Instron test machine (Model 5566, load cell capacity of 100 N, Grove City, PA) was used to test the mechanical properties of the films. The crosshead speed was 10 mm/min and the crosshead extension was used as specimen deformation. All samples were cut to dog-bone shapes with widths of 5 mm and lengths of 20 mm for the narrow portions. Five specimens for each MFC level film were tested in accordance to ASTM D1708 [58]. Tensile elastic modulus of all films was determined from the linear portion of the stress-strain curves. Multiple comparisons by the Statistical Analysis System (SAS) (t-tests (LSD)) were used to detect the overall significant differences of MFC influences on the tensile elastic modulus and strength of composites ($\alpha = 0.05$).

A thermogravimetric analyzer (TGA/DSC1, Stare system, Mettler Toledo, Schwerzenbach, Switzerland) was used to determine the thermal behaviors of the

PVA MFC nanocomposite films, neat PVA and neat MFC. The sample weight was approximately 10 mg and heated from 50 °C to 500 °C at a 20 °C/min heating rate. The tests were conducted under nitrogen gas with a flow rate of 20 ml/min to avoid oxidation. Scanning electron microscopy (SEM; same process was used as described above) was also used to examine the topography of sample fracture surfaces after tensile test.

3   Results and Discussion

3.1   SEM Observation of MFC

Figure 22.7 shows the SEM images of MFC in micro- and nanoscales. The MFC diameters were ranged from tens of nanometer (nm) up to approximately hundreds of nm, but most of them were less than 100 nm. The MFC lengths were ranged from several micrometers (μm) up to tens of μm. It is estimated that the MFC aspect ratio (length/diameter) could be up to 100. Microfibers and nanofibers with high aspect ratios could greatly improve the mechanical properties of neat PVA [2, 4, 36].
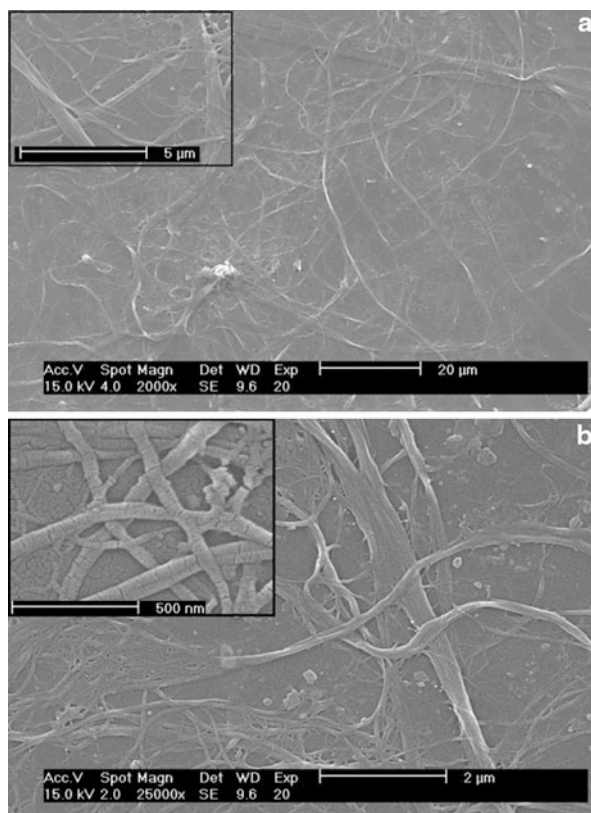

Fig. 22.7 SEM images of microfibrillated cellulose (MFC) with low ((**a**) scale = 20 μm and the insert scale = 5 μm) and high ((**b**) scale = 2 μm and the insert scale = 500 nm) magnifications
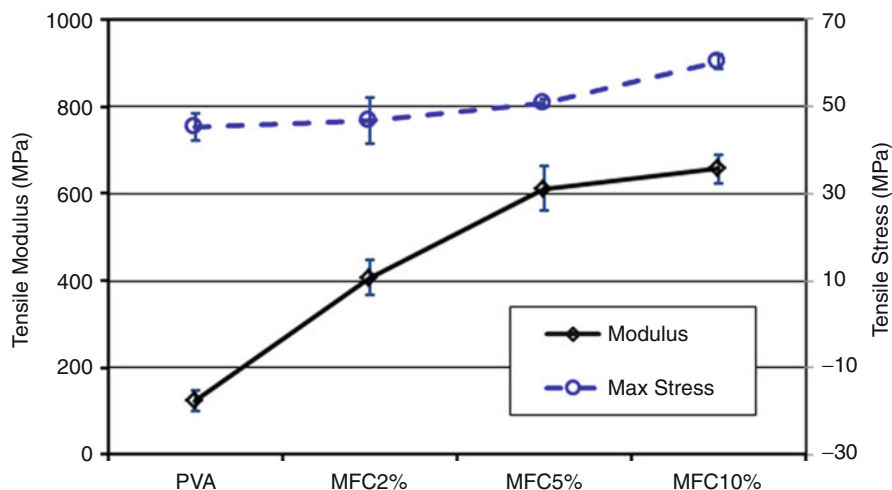
Fig. 22.8 Tensile modulus and max stress of PVA and PVA MFC nanocomposites with 2 %, 5 %, and 10 % MFC loadings

Table 22.1 Statistical analysis data of tensile modulus, max stress, and max strain at break of PVA and its MFC nanocomposites with 2 %, 5 %, and 10 % MFC loadings

Sample	Specimen number	Max stress (MPa)		Modulus (MPa)		Max strain (%)	
		Mean	t grouping[a]	Mean	t grouping[a]	Mean	t grouping[a]
PVA	5	45.3	C	123.4	C	3.63	A
MFC2	5	46.8	BC	406.8	B	2.68	B
MFC5	5	50.9	B	611.8	A	1.59	C
MFC10	5	60.2	A	656.4	A	0.69	D

[a]Means with the same letter are not significantly different

3.2   Tensile Mechanical Properties of the Nanocomposites

Figure 22.8 shows the tensile moduli and tensile strengths (max stress) of neat PVA and PVA MFC nanocomposites with 2, 5, and 10 wt% MFC loadings, and the statistical analysis data are shown in Table 22.1. The tensile modulus of neat PVA was increased 230 %, 396 %, and 432 % in the substitution of 2 %, 5 %, and 10 wt% MFC, respectively. These results indicated that MFC could significantly improve PVA modulus. The modulus increased with the enhancement of MFC loading levels. However, as the substitution of 10 wt% of MFC, the modulus of MFC composite was not significantly different with that of MFC composite with 5 wt% (Fig. 22.8, Table 22.1). This is partially caused by the aggregation of small fibrils at a high fibril loading. It has been reported that the aggregation of smaller cellulose fibrils under a high loading level of fibrils may affect the reinforcement of their composites [4, 38].
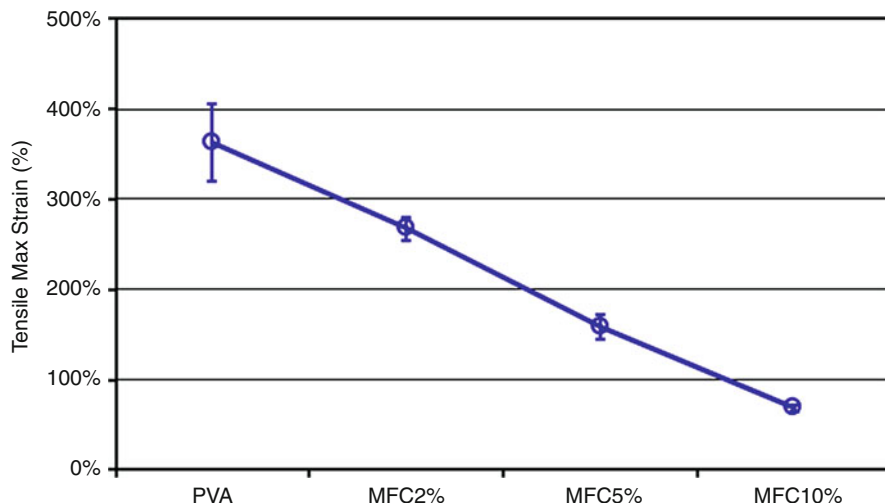
Fig. 22.9 Tensile max strain at break of PVA and PVA MFC nanocomposites with 2 %, 5 %, and 10 % MFC loadings

The tensile strength (max stress) of neat PVA could also be improved as the substitution of MFC, and it increased with the enhancement of MFC loading levels. Although the substitution of 2 wt% MFC did not significantly increase the tensile strength of neat PVA, at a 5 wt% and 10 wt% loading level, the tensile strengths were significantly improved according to the statistical analysis under 95 % confidence ($\alpha = 0.05$ %) (Table 22.1). The reinforcement could be attributed to a high aspect ratio of MFC.

Figure 22.9 shows the tensile max strain (elongation) of neat PVA and PVA MFC nanocomposites as the substitution of 2, 5, and 10 wt% of MFC. The max strain at break of neat PVA was significantly decreased by all three MFC loadings, and it was decreased with the incensement of the MFC loading levels (Fig. 22.9, Table 22.1). It may be caused by the brittle property of MFC, the aggregation of small-sized MFC, and the uneven MFC distribution in the polymer matrix [4, 38].

3.3   Thermal Properties of the Nanocomposites

Thermal properties of neat PVA and the PVA MFC nanocomposites were analyzed using thermogravimetric analysis (TGA). The TGA and derivative TGA (DTGA) thermograms are shown in Fig. 22.10. Basically, we observed three weight-loss regions. The first region exhibited an initial weight loss from 70 °C to 150 °C due to the evaporation of water. The second degradation region was the max weight-loss region from 250 °C to 400 °C with a weight loss from 50 % to 75 % depending on the different materials, which were mainly attributed to the degradation of the PVA
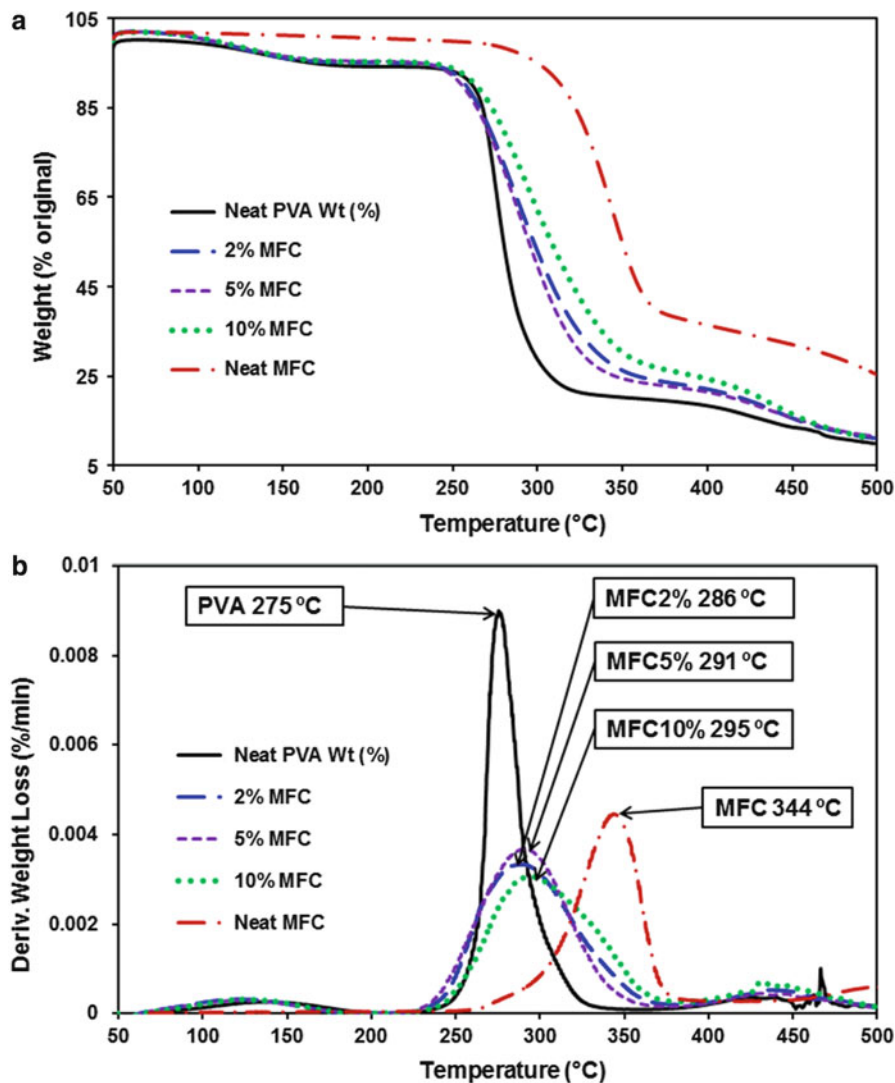
Fig. 22.10 TGA (**a**) and DTGA (**b**) diagrams of neat PVA, MFC, and PVA MFC nanocomposites with 2 %, 5 %, and 10 % MFC loadings

and its composites. The third region of weight loss occurred above 400 °C, which was mainly caused by the decomposition of carbonaceous matters from the PVA and cellulose [59, 60].

Water content has significant effects on the mechanical properties. The water content of MFC was lower than PVA and its composites because it was not conditioned after drying. The PVA and all nanocomposites had relative high water contents (~2 %) since they were conditioned at the RH of 53 % for more

than 3 days (Fig. 22.10a). The water has strong plasticizing effect and improves the movement of PVA chains [60]. This could be the main reason that the tensile modulus and strength shown in Fig. 22.8 were not as high as those of PVA and its composites without 50 % RH conditioning [4].

Neat PVA thermally degraded at a lower temperature than neat MFC (Fig. 22.10a). The PVA/MFC nanocomposites had a lower degradation temperature than the neat MFC but a higher temperature than the neat PVA. DTGA curves further confirm these results (Fig. 22.10b). As shown in Fig. 22.10, the max degradation temperature of PVA was increased about 11 °C, 16 °C, and 20 °C by adding 2 %, 5 %, and 10 % MFC, respectively. It was caused by the higher degradation temperature of cellulose (315–400 °C) compared to that of polyvinyl alcohol (200–300 °C) [61, 62].

3.4   SEM Observation of the Composites Fracture Surfaces

The SEM images of fractured cross sections of PVA and its MFC nanocomposites after tensile test are shown in Fig. 22.11. It was observed that the fracture surfaces of nanocomposites were rough (Fig. 22.11a–c) compared to the relatively smooth surface of the neat PVA film (Fig. 22.11d). The MFC fibrils were well dispersed in the PVA matrix, but they were not uniformly distributed in the matrix (Fig. 22.11c).
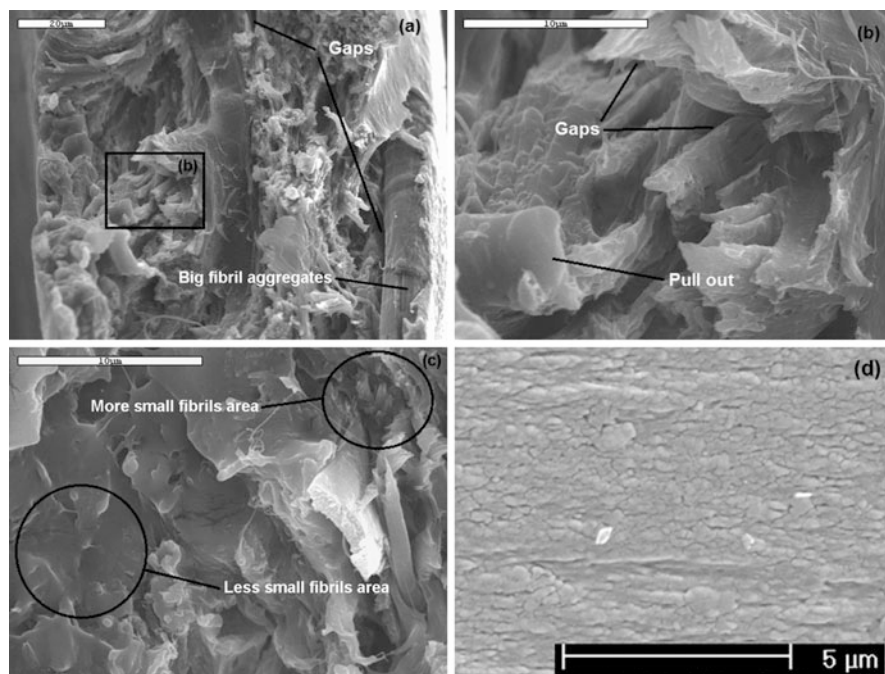

Fig. 22.11 SEM images of the fractured cross sections of PVA MFC nanocomposites with 5 % MFC loading ((**a**) scale = 20 μm; (**b**) scale = 10 μm; (**c**) scale = 10 μm) and neat PVA (**d**)

There were some clear gaps between MFC fibrils (especially large fibril aggregations) and the PVA matrix (Fig. 22.11a, b). Some MFC fibrils could be pulled out during tensile test (Fig. 22.11b). These could be the main reasons that the tensile strength (max stress) of PVA was not increased much by adding MFC and the max strain at break of the MFC nanocomposites was significantly decreased compared with neat PVA (Fig. 22.8) [4].

4   Conclusions

Cellulose fibrils in micro- and nanoscales (nanofibers or nanocrystals) can be generated by mechanical or chemical methods. Both cellulose nanofibers and nanocrystals can be used to reinforce PVA to produce biodegradable nanocomposites by film casting methods. Commercial microfibrillated cellulose (MFC) with diameters ranged from tens of nanometer to hundreds of nm was used to reinforce PVA in this chapter as an example. Both tensile modulus and tensile strength of neat PVA were significantly improved with the substitution of the MFC from 2 wt% to 5 wt%. However, the PVA max tensile strain was decreased significantly. Thermal gravimetric data revealed that the MFC-reinforced nanocomposites had higher thermal degradation temperatures compared with neat PVA. The entire nanocomposites are biodegradable and environmentally friendly.

References

1. Jordan J, Jacob KI, Tannenbaum R, Sharaf MA, Jasiuk I (2005) Mater Sci Eng A Struct Mater Prop Microstruct Process 393:1
2. Chakraborty A, Sain M, Kortschot M (2006) Holzforschung 60:53
3. Cheng Q, Wang S, Harper D (2009) Comp A Appl Sci Manuf 40:583
4. Cheng Q, Wang S, Rials T (2009) Comp A Appl Sci Manuf 40:218
5. Gea S, Bilotti E, Reynolds CT, Soykeabkeaw N, Peijs T (2010) Mater Lett 64:901
6. Qiu K, Netravali AN (2012) J Mater Sci 47:6066
7. Finch CA (1987) Poly(vinyl alcohol): properties and applications. Wiley, New York
8. Hassan CM, Peppas AN (2000) Adv Polym Sci 153:37–65
9. Wise LE, Murphy M, Addieco AA (1946) Pap Trade J 122:35
10. Kamphunthong W, Hornsby P, Sirisinha K (2012) J Appl Polym Sci 125:1642
11. Wang J, Cheng Q, Adebayo AB, Difazio S (2012) Poly(vinyl alcohol) nanocomposites reinforced with cellulosic nanofibers isolated from juvenile poplar. In: Cheng Q (ed) Fiber-reinforced composites. Nova Science, New York, p 91
12. Choi YJ, Simonsen J (2006) J Nanosci Nanotechnol 6:633
13. Sakurada I, Nukushina Y, Ito T (1962) J Polym Sci 57:651
14. Dufresne A, Cavaille JY, Vignon MR (1997) J Appl Polym Sci 64:1185
15. Edgar CD, Gray DG (2002) Macromolecules 35:7400
16. Zimmermann T, Pohler E, Geiger T (2004) Adv Eng Mater 6:754

17. Beck-Candanedo S, Roman M, Gray DG (2005) Biomacromolecules 6:1048
18. Chakraborty A, Sain M, Kortschot M (2005) Holzforschung 59:102
19. Kvien I, Tanem BS, Oksman K (2005) Biomacromolecules 6:3160
20. Lu YS, Weng LH, Cao XD (2005) Macromol Biosci 5:1101
21. Pu Y, Zhang J, Elder T, Deng Y, Gatenholm P, Ragauskas A (2007) Comp B Engine 38:360
22. Peresin MS, Habibi Y, Zoppe JO, Pawlak JJ, Rojas OJ (2010) Biomacromolecules 11:674
23. Cho MJ, Park BD (2011) J Ind Eng Chem 17:36–40
24. Uddin AJ, Araki J, Gotoh Y (2011) Biomacromolecules 12:617
25. Uddin AJ, Araki J, Gotoh Y (2011) Comp A Appl Sci Manuf 42:741
26. Uddin AJ, Araki J, Gotoh Y (2011) Polym Int 60:1230
27. Herrick FW, Casebier RL, Hamilton JK, Sandberg KR (1983) J Appl Polym Sci Appl Polym Symp 37:797
28. Turbak AF, Snyder FW, Sandberg KR (1983) J Appl Polym Sci Appl Polym Symp 37:815
29. Taniguchi T, Okamura K (1998) Polym Int 47:291
30. Wang S, Cheng Q (2009) J Appl Poly Sci 113:1270
31. Cheng Q, Wang S, Han Q (2010) J Appl Poly Sci 115:2756
32. Li W, Yue J, Liu S (2012) Ultrason Sonochem 19:479
33. Abramov O (1998) High-intensity ultrasonic theory and industrial applications. Gordon and Breach Science Publishers, Amsterdam
34. Bhatnagar A, Sain M (2005) J Reinf Plast Comp 24:1259
35. Bondeson D, Mathew A, Oksman K (2006) Cellulose 13:171
36. Wang B, Sain M (2007) Compos Sci Technol 67:2521
37. Yano H, Nakahara S (2004) J Mater Sci 39:1635
38. Cheng Q, Wang S, Rials T, Lee SH (2007) Cellulose 14:593
39. Cheng Q, Wang J, McNeel J, Jacobson P (2010) BioResources 5:1945
40. Gindl W, Keckes J (2005) Polymer 46:10221
41. Wiley JH, Atalla RH (1987) Carbohydr Res 160:113
42. Matsuo M (1990) Macromolecules 23:13
43. Tan EPS, Lim CT (2004) Appl Phys Lett 84:1603
44. Wan WK, Hutter JL, Millon L, Guhados G (2006) Bacterial cellulose and its nanocomposites for biomedical applications. In: Oksman K, Sain M (eds) Cellulose nanocomposites: processing, characterization, and properties. American Chemical Society, Washington, DC, p 221
45. Cheng Q, Wang S (2008) Comp A Appl Sci Manuf 39:1838
46. Favier V, Canova GR, Cavaillé JY, Chanzy H, Dufresne A, Gauthier C (1995) Polym Adv Technol 6:351
47. Dufresne A, Cavaille J, Helbert W (1997) Polym Comp 18:198
48. Iwamoto S, Nakagaito AN, Yano H, Nogi M (2005) Appl Phys A Mater Sci Process 81:1109
49. Nakagaito AN, Yano H (2005) Appl Phys A Mater Sci Process 80:155
50. Cheng Q, Wang S, Zhou D, Zhang Y, Rials T (2007) J Nanjing Forestry Univ 31:21
51. Zimmermann T, Pohler E, Schwaller P (2005) Adv Eng Mater 7:1156
52. Peresin MS, Habibi Y, Vesterinen AH, Rojas OJ, Pawlak JJ, Seppala JV (2010) Biomacromolecules 11:2471
53. Srithep Y, Turng LS, Sabo R, Clemons C (2012) Cellulose 19:1209
54. Orts WJ, Shey J, Imam SH, Glenn GM, Guttman ME, Revo JF (2005) J Polym Environ 13:301
55. Ljungberg N, Cavaille JY, Heux L (2006) Polymer 47:6285
56. Samir M, Alloin F, Dufresne A (2006) Compos Interfac 13:545
57. Kadokawa J, Takegawa A, Mine S, Prasad K (2011) Carbohydr Polym 84:1408
58. ASTM (2002) American Society for Testing and Materials, West Conshohocken. D 1708–2002a
59. Lee SY, Mohan DJ, Kang IA, Doh DH, Lee S, Han SO (2009) Fibers Polym 10:77
60. Frone AN, Panaitescu DM, Donescu D, Spataru CI, Radovici D, Trusca R (2011) BioResources 6:487
61. Yang H, Yan R, Chen H, Lee DH, Zheng C (2007) Fuel 86:1781
62. Holland BJ, Hay JN (2011) Polymer 42:6775